Cement & Concrete Composites 34 (2012) 716–723

Contents lists available at SciVerse ScienceDirect

Cement & Concrete Composites

journal homepage: www.elsevier.com/locate/cemconcomp

An *n*-layered spherical inclusion model for predicting the elastic moduli of concrete with inhomogeneous ITZ

Jianjun Zheng [a,*], Xinzhu Zhou [a], Xianyu Jin [b]

[a] School of Civil Engineering and Architecture, Zhejiang University of Technology, Hangzhou 310014, PR China
[b] School of Civil Engineering and Architecture, Zhejiang University, Hangzhou 310058, PR China

ARTICLE INFO

Article history:
Received 31 January 2010
Received in revised form 26 January 2012
Accepted 27 January 2012
Available online 4 February 2012

Keywords:
Concrete
Elastic moduli
n-Layered spherical inclusion model
Inhomogeneous interfacial transition zone

ABSTRACT

An *n*-layered spherical inclusion model is presented in this paper for predicting the elastic moduli of concrete with inhomogeneous interfacial transition zone (ITZ). In this model, concrete is represented as a three-phase composite material, composed of the aggregate, bulk paste, and an inhomogeneous ITZ. An analytical solution for the ITZ volume fraction is derived for the general aggregate gradation. By constituting a semi-empirical initial cement gradient model, the local water/cement ratio, degree of hydration, and porosity at the ITZ are estimated. The inhomogeneous ITZ is then divided into a series of homogenous concentric shell elements of equal thickness. The elastic moduli of concrete are determined by solving the *n*-layered spherical inclusion problem. Finally, the validity of the model is verified with three independent sets of experimental data and the effects of the maximum aggregate diameter, aggregate gradation, and ITZ thickness on the Young's modulus of concrete are evaluated in a quantitative manner. The paper concludes that the proposed *n*-layered spherical inclusion model can be used to predict the elastic moduli of concrete.

1. Introduction

Elastic moduli of concrete play an essential role in the design and assessment of concrete structures and have therefore been studied extensively, both experimentally and theoretically [1–9]. It has been shown that, when the cement grains encounter the "wall" of the aggregate, an interfacial transition zone (ITZ) with a significantly higher porosity near the aggregate surface will appear, due to the "packing" constraints imposed by the aggregate surface [10–12]. This fact implies that the ITZ should be considered to be an independent phase in predicting the physicomechanical properties of concrete. Therefore, numerous theoretical efforts have been made to correlate the macroscopic elastic moduli of concrete with the volume fraction, morphology, and mechanical properties of each phase constituent [4–9].

Owing to the distinctive microstructure of the ITZ [10–12], concrete should be modeled as a three-phase composite material and can be represented by a three-phase composite sphere assemblage at a mesoscopic level [6,9]. Dividing each three-phase composite sphere into 2 two-phase composite spheres and applying Christensen's formula for the effective bulk modulus of two-phase composite materials [13], Li et al. obtained the elastic moduli of concrete [6]. In their solution, however, the overlaps between the ITZs were neglected and the interaction of the three phase constituents was not fully considered, which would inevitably influence the accuracy of the prediction. To improve this, Zheng et al. proposed a three-phase composite circle model for the elastic moduli of concrete [9], in which the overlaps between ITZs was considered in estimating the ITZ area fraction and the effective bulk modulus of concrete was directly derived by solving the three-phase composite circle problem. Besides purely analytical methods, numerical simulations are also an ideal tool. With the simulated distribution of circular aggregates and ITZs within a rectangular element, the heterogeneity of concrete and the overlaps between the ITZs can realistically be generated [7]. The finite element method was then employed to determine the Young's modulus. One obvious disadvantage of the numerical simulation is that it requires heavy computational means. It should be pointed out that, in the above methods, the ITZ is all assumed to be homogeneous. To take into account the inhomogeneity of the ITZ, Lutz et al. approximated the elastic moduli of ITZ as a power-law function of radial distance from the center of the aggregate and derived an analytical solution for the bulk modulus of concrete [5]. However, it is still extremely difficult to formulate the shear modulus of concrete due to mathematical complexity. Nadeau proposed a multi-scale model for the elastic moduli of concrete by incorporating the local water/cement ratio at the ITZ [8]. The main limitations of this method are that the cement volume fraction at the interface between the aggregate and ITZ was taken as

* Corresponding author. Tel.: +86 571 88320847; fax: +86 571 88320460.
E-mail address: jjzheng@zjut.edu.cn (J. Zheng).

0958-9465/$ - see front matter © 2012 Elsevier Ltd. All rights reserved.
doi:10.1016/j.cemconcomp.2012.01.011

half that in the bulk paste, which does not seem to be consistent with the experimental observations of Crumbie [11], and that the overlaps between ITZs were neglected in evaluating the cement volume fraction of bulk paste. All of the above references clearly show that the existing prediction methods have two main limitations. First, the ITZ layer is assumed to be uniform in most models and the mechanical properties of the bulk paste away from the aggregate surface are usually replaced with those of the neat cement paste without aggregate. Thus, the effect of the ITZ on the water/cement ratio in and elastic moduli of bulk paste is neglected. Second, the initial cement gradient at the ITZ is not taken into account in a proper manner. Therefore, it is still desirable to develop a numerical method to predict the elastic moduli of concrete with inhomogeneous ITZ more reasonably and efficiently.

The intention of this paper is to present an n-layered spherical model for predicting the elastic moduli of concrete with inhomogeneous ITZ. By representing concrete as a three-phase composite material and constituting a semi-empirical cement gradient model, the local water/cement ratio, degree of hydration, porosity, and elastic moduli at the ITZ are estimated. By dividing the inhomogeneous ITZ into a series of homogenous concentric shell elements, the elastic moduli of concrete are determined by solving the n-layered spherical inclusion problem. After the validity of the proposed model is verified with three independent sets of experimental data, the effects of three main influential factors on the Young's modulus of concrete are investigated through sensitivity analysis.

2. ITZ volume fraction in concrete with general aggregate gradation

When the ITZ is treated as an independent phase, concrete should be modeled as a three-phase material and is further conceptualized as a space filling assemblage of three-phase composite spheres of various sizes. For a typical three-phase composite sphere shown in Fig. 1a, r_a denotes the radius of the aggregate, $r_b - r_a$ the thickness of the ITZ layer, and $r_c - r_b$ the thickness of the bulk paste. To represent the concrete of practical use, the proportion of each phase constituent in the composite sphere should satisfy the following conditions [4]

$$\frac{r_a^3}{r_c^3} = f_{agg} \tag{1a}$$

$$\frac{r_b^3}{r_c^3} = f_{agg} + f_{itz} \tag{1b}$$

where f_{agg} and f_{itz} are the volume fractions of aggregate and ITZ, respectively. Since the aggregate volume fraction is given beforehand, the key effort in making the composite sphere model workable is to determine the ITZ volume fraction. For this purpose, it is assumed in this paper that aggregates are spherical and divided into L grades $[D_j, D_{j+1}]$ ($j = 1, 2, \ldots, L$), where D_1 and D_{L+1} are the minimum and maximum aggregate diameters, respectively. The cumulative volume percentage $P_V(D_j)$ passing the sieve with diameter D_j can be obtained by sieve analysis. If the cumulative volume percentage is approximated as a piecewise linear function, the probability density function $p_V(D)$ for the aggregates in terms of the volume of aggregates can be expressed as

$$p_V(D) = \sum_{j=1}^{L} \frac{[P_V(D_{j+1}) - P_V(D_j)]}{D_{j+1} - D_j} [H(D - D_j) - H(D - D_{j+1})] \tag{2}$$

where the Heaviside step function $H(D - D_j)$ is defined as

$$H(D - D_j) = \begin{cases} 0, D < D_j \\ 0.5, D = D_j \\ 1, D > D_j \end{cases} \tag{3}$$

The probability density function $p_N(D)$ for the aggregates in terms of the number of aggregates is related to $p_V(D)$ by

$$\begin{aligned} p_N(D) &= \frac{p_V(D)}{(\pi/6)D^3 N_V} \\ &= \sum_{j=1}^{L} \frac{6[P_V(D_{j+1}) - P_V(D_j)]}{\pi N_V (D_{j+1} - D_j) D^3} [H(D - D_j) - H(D - D_{j+1})] \end{aligned} \tag{4}$$

where N_V is the number of aggregates per unit volume of aggregate and given by

$$N_V = \int_{D_1}^{D_{L+1}} \frac{p_V(D)dD}{(\pi/6)D^3} = \sum_{j=1}^{L} \frac{3(D_j + D_{j+1})[P_V(D_{j+1}) - P_V(D_j)]}{\pi D_j^2 D_{j+1}^2} \tag{5}$$

The kth moment $\langle D^k \rangle$ of area of $p_N(D)$ about the origin is defined as [14]

$$\langle D^k \rangle = \int_{D_1}^{D_{L+1}} D^k p_N(D) dD \tag{6}$$

Substitution of Eq. (4) into Eq. (6) yields

$$\langle D^k \rangle = \begin{cases} \sum_{j=1}^{L} \frac{6[P_V(D_{j+1}) - P_V(D_j)] \ln(D_{j+1}/D_j)}{\pi N_V (D_{j+1} - D_j)}, & \text{for } k = 2 \\ \sum_{j=1}^{L} \frac{6[P_V(D_{j+1}) - P_V(D_j)](D_{j+1}^{k-2} - D_j^{k-2})}{(k-2)\pi N_V (D_{j+1} - D_j)}, & \text{otherwise} \end{cases} \tag{7}$$

It has been recognized that the wall effect leads to an initial cement gradient at the ITZ. Due to a lack of experimental data, to what extent the aggregate size affects the ITZ thickness and the initial cement gradient at the ITZ is still an open issue. Therefore, it is assumed in this paper that, as a preliminary study, the ITZ thickness and the initial cement gradient at the ITZ are both independent of the aggregate size. In evaluating the ITZ volume fraction,

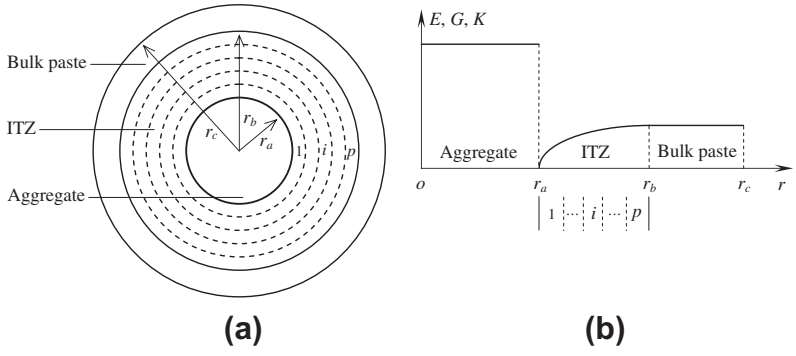

Fig. 1. (a) Spherical shell element discretization of ITZ layer; (b) Variation of elastic moduli along the radial direction.

the overlaps between the ITZs need to be taken into account. This can be achieved analytically using the 'void exclusion probability' derived by Lu and Torquato [15] for the polydispersed spheres system, and as described in Bentz and Garboczi [4]. When applied to the current case, the void exclusion probability is basically the volume fraction of the space not occupied by all the spherical aggregates and ITZ shells, i.e., fraction of bulk paste. Accordingly, the ITZ volume fraction f_{itz} can be expressed as

$$f_{itz} = (1 - f_{agg})[1 - \exp(-t_1 h - t_2 h^2 - t_3 h^3)] \tag{8}$$

where h is the ITZ thickness, and t_1, t_2, and t_3 are respectively defined in terms of f_{agg} and $\langle D^k \rangle$ as

$$t_1 = \frac{6 f_{agg} \langle D^2 \rangle}{(1 - f_{agg}) \langle D^3 \rangle} \tag{9a}$$

$$t_2 = \frac{12 f_{agg} \langle D \rangle}{(1 - f_{agg}) \langle D^3 \rangle} + \frac{18 f_{agg}^2 \langle D^2 \rangle^2}{(1 - f_{agg})^2 \langle D^3 \rangle^2} \tag{9b}$$

$$t_3 = \frac{8 f_{agg}}{(1 - f_{agg}) \langle D^3 \rangle} + \frac{24 f_{agg}^2 \langle D \rangle \langle D^2 \rangle}{(1 - f_{agg})^2 \langle D^3 \rangle^2} + \frac{8\omega f_{agg}^3 \langle D^2 \rangle^3}{(1 - f_{agg})^3 \langle D^3 \rangle^3} \tag{9c}$$

with ω being equal to 2, 3, and 0 for the Carnahan-Starling, scaled-particle, and Percus–Yevick approximation, respectively [15]. By comparison with numerically exact model data, Garboczi and Bentz concluded that $\omega = 0$ is always the best choice to use [4]. Thus ω is taken as zero in this paper. Once the ITZ volume fraction is known, the volume fraction of bulk paste f_{bulk} is obtained by simple subtraction.

3. Porosity gradient at ITZ

Due to the effect of the aggregate surface on the distribution of cement grains, an initial cement gradient is formed at the ITZ. Crumbie measured the distributions of the anhydrous cement, porosity, and hydration products after various hydration times using backscattered electron microscopy [11]. In calculating the initial cement gradient, he assumed that the hydration products deposit close to the anhydrous cement particle from which they form. Although there is evidence that C–S–H forms 'through solution', the low mobility of the silicate ions in solution means that this assumption is probably valid to a first approximation at 1 day. Based on the experimental results, the volume ratio of the anhydrous cement hydrated to hydration products formed was calculated at 1 day, 28 days, and 1 year. Since the volume ratio at 1 day is least affected by migration, he used this value to back-calculate the initial cement gradient for concretes with different water/cement ratios as shown in Fig. 2. Using the data shown in Fig. 2, the initial cement gradient $f_c(r)$ can approximately be expressed as

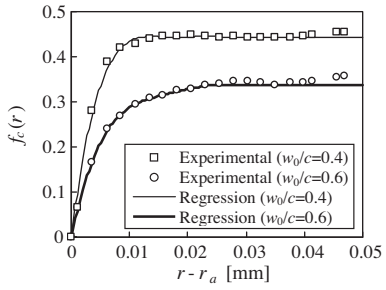

Fig. 2. Comparison between regression results and experimental results of Crumbie [11].

$$f_c(r) = \begin{cases} f_{c,bulk} \sum_{j=1}^{4} (b_j/b_0)[(r - r_a)/(r_b - r_a)]^j, r_a \leqslant r < r_b \\ f_{c,bulk}, r_b \leqslant r \leqslant r_c \end{cases} \tag{10}$$

where $f_{c,bulk}$ is the cement volume fraction in the bulk paste, r is the distance from the center of the aggregate, b_0 is the sum of b_j (i.e., $b_0 = b_1 + b_2 + b_3 + b_4$), and b_j is a series of empirical functions in terms of w_0/c and can be obtained from least squares analysis that

$$\begin{aligned} b_1 &= 4.670 - 5.228(w_0/c) \\ b_2 &= -10.569 + 12.700(w_0/c) \\ b_3 &= 9.950 - 12.195(w_0/c) \\ b_4 &= -3.397 + 4.195(w_0/c) \end{aligned} \tag{11}$$

According to the conservation of cement volume, the total cement volume V_c in the composite sphere is the sum of the cement volume $V_{c,itz}$ in the ITZ and the cement volume $V_{c,bulk}$ in the bulk paste

$$V_c = V_{c,itz} + V_{c,bulk} \tag{12}$$

V_c is expressed as

$$V_c = \frac{4\pi(r_c^3 - r_a^3)}{3[1 + \rho_c(w_0/c)]} \tag{13a}$$

where ρ_c is the cement density. $V_{c,bulk}$ is the product of $f_{c,bulk}$ and the volume of the bulk paste

$$V_{c,bulk} = \frac{4\pi(r_c^3 - r_b^3) f_{c,bulk}}{3} \tag{13b}$$

and $V_{c,itz}$ can be obtained by integrating Eq. (10) from $r = r_a$ to r_b that

$$V_{c,itz} = 8\pi f_{c,bulk} \sum_{j=1}^{4} \sum_{k=1}^{3} \frac{b_j r_a^{(3-k)} (r_b - r_a)^k}{b_0 (j+k)[(k-1)!][(3-k)!]} \tag{13c}$$

By substituting Eq. (13) into Eq. (12), $f_{c,bulk}$ is given by

$$f_{c,bulk} = \frac{(r_c^3 - r_a^3)}{[1 + \rho_c(w_0/c)]\left[(r_c^3 - r_b^3) + 6\pi \sum_{j=1}^{4} \sum_{k=1}^{3} \frac{b_j r_a^{(3-k)} (r_b - r_a)^k}{b_0 (j+k)[(k-1)!][(3-k)!]}\right]} \tag{14}$$

Fig. 2 shows the agreement between Eq. (10) and the data from Crumbie [11]. The correlation coefficients for the regression analysis are 0.9982 and 0.9978 for w_0/c of 0.4 and 0.6, respectively. It should be pointed out that, due to the wall effect, the initial cement gradient is affected by the water/cement ratio and the particle size distribution of cement. b_1, b_2, b_3, and b_4 in Eq. (11) are obtained based on the experimental results of Crumbie [11] and therefore are likely to be less accurate for other particle size distributions of cement. Because of a lack of relevant experimental data, Eq. (11) is assumed to be valid for other particle size distributions of cement as a preliminary study.

The local water/cement ratio w/c at the ITZ is given by

$$w/c = \frac{1 - f_c(r)}{\rho_c f_c(r)} \tag{15}$$

Thus the degree of hydration α is also a function of r and can be estimated by Parrot and Killoh's approach [16]. As the cement hydrates, the originally water-filled spaces (capillary pores) become progressively filled with hydration products due to increase in total solids volume. However, the main hydration product (C–S–H) also contains pores, i.e., gel pores, and these will increase in volume as hydration continues. According to Powers' empirical model [17], the capillary volume fraction f_{cap} and the gel volume fraction f_{gel} are related to the water/cement ratio and the degree of hydration, hence the total porosity f_p is

$$f_p = f_{cap} + f_{gel} = \frac{(w/c) - 0.36\alpha}{(w/c) + 0.32} + \frac{0.19\alpha}{(w/c) + 0.32} \tag{16}$$

It should be pointed out that Eq. (16) was derived using specific values of chemical and physical bound water, and chemical shrinkage for the hydration of typical Portland cements under room temperature conditions [17]. Thus, Eq. (16) is likely to be less accurate for other systems such as those containing supplementary cementitious materials.

4. *n*-Layered spherical inclusion model for the elastic moduli of concrete

In predicting its elastic moduli, it is assumed in this paper that concrete is a homogeneous, isotropic elastic material. Since the porosity at the ITZ varies not only with the water/cement ratio and the degree of hydration, but also with the distance from the aggregate surface as seen from Eqs. (15) and (16), it is extremely difficult to describe the variation of the cement paste elastic moduli through the ITZ by a simple analytic function, let alone to derive the elastic moduli of concrete in an analytical manner. In view of this difficulty, an *n*-layered spherical inclusion model is presented in this paper. In this model, the inhomogeneous ITZ is divided into a series of homogeneous and isotropic concentric shell elements. The elastic moduli of these ITZ shell elements are determined by modeling them as a two-phase composite material, composed of a solid cement paste and pores. With these inputs, the elastic moduli of concrete are then evaluated by solving the *n*-layered spherical inclusion problem, in which only a two-phase composite sphere problem needs to be solved at each step. Therefore, it is essential to select a high accuracy yet simple analytical solution for the effective elastic moduli of two-phase composite materials. For this purpose, the two-phase composite material is represented by a two-phase composite sphere assemblage. For a typical composite sphere shown in Fig. 3, the inner sphere is inclusion phase i and the outer spherical shell is matrix phase m. If K, G, E, and v with subscript notation denote the bulk modulus, shear modulus, Young's modulus, and Poisson's ratio of concrete or any individual phase constituent within it, the effective bulk modulus K_e of the two-phase composite material can be expressed as [13]

$$K_e = K_m + \frac{(K_i - K_m)f_i}{1 + [(1 - f_i)(K_i - K_m)/(K_m + 4G_m/3)]} \tag{17}$$

where f_i is the volume fraction of inclusion phase i. As for the effective shear modulus of the two-phase composite material, the analytical solution derived by Duan et al. is adopted in this paper [18]. Compared with Christensen and Lo's solution [19], Duan et al.'s one is almost of the same accuracy but has a more concise expression. According to Duan et al. [18], the effective shear modulus G_e is given by

$$G_e = \frac{B - \sqrt{B^2 - 4AC}}{2A} G_m \tag{18}$$

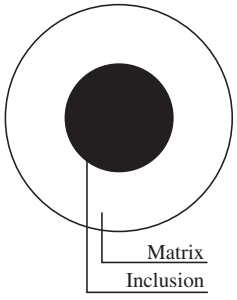

Fig. 3. Two-phase composite sphere model.

where

$$\begin{aligned} A &= -[126f_i^{7/3} - 252f_i^{5/3} + 50(7 - 12\nu_m + 8\nu_m^2)f_i](1 - G_i/G_m) + 4(7 - 10\nu_m)g \\ B &= -[252f_i^{7/3} - 504f_i^{5/3} + 150(3 - \nu_m)\nu_m f_i](1 - G_i/G_m) + 3(7 - 15\nu_m)g \\ C &= -[126f_i^{7/3} - 252f_i^{5/3} + 25(7 - \nu_m^2)f_i](1 - G_i/G_m) - (7 + 5\nu_m)g \end{aligned} \tag{19}$$

with

$$g = -7 + 5\nu_m - 2(G_i/G_m)(4 - 5\nu_m) \tag{20}$$

As stated above, the inhomogeneous ITZ is divided into p concentric shell elements of equal thickness as shown in Fig. 1b. Each shell element is further idealized as a two-phase composite sphere assemblage and the pores within the element are taken as spherical inclusions as shown in Fig. 3. Since the porosity of the ITZ shell element can be calculated from Eq. (16), the key effort in obtaining the elastic moduli of the ITZ shell element is to determine the elastic moduli K_{scp}, G_{scp}, E_{scp}, and ν_{scp} of the solid cement paste matrix. Although it is appreciated that the elastic moduli of the solid cement paste can be estimated analytically by the homogenization technique [20,21], these analytical methods are computationally complicated. Therefore, experimental calibration seems to be a more simple, convenient and practical method. In this method, a neat cement paste made with the same cement after the same hydration time as the concrete is selected and idealized as a two-phase composite sphere assemblage as the ITZ shell element. The shear modulus G_{pore} of the pore water is taken as zero [22]. The bulk modulus K_{pore} of the pore water is closely related to the degree of saturation. In view of the difficulty in identifying the degree of saturation in some practical applications, only two extreme cases are considered in this paper: when the pores are fully saturated, K_{pore} is equal to 2.2 GPa, otherwise K_{pore} is taken as zero [23]. The porosity f_{ncp} is calculated from Eq. (16). It follows from Eqs. (17) and (18) that

$$K_{ncp} = K_{scp} - \frac{f_{ncp}K_{scp}}{1 - (1 - f_{ncp})K_{scp}/(K_{scp} + 4G_{scp}/3)} \tag{21}$$

$$G_{ncp} = \frac{B - \sqrt{B^2 - 4AC}}{2A} G_{scp} \tag{22}$$

where K_{ncp} and G_{ncp} are the bulk modulus and shear modulus of the neat cement paste, and A, B, and C are obtained from Eq. (19) by replacing f_i, ν_m, G_i, and G_m with f_{ncp}, ν_{scp}, G_{pore}, and G_{scp}, respectively. In addition, according to the theory of elasticity [24], G_{scp} is related to K_{scp} and ν_{scp} by

$$G_{scp} = \frac{3(1 - 2\nu_{scp})}{2(1 + \nu_{scp})} K_{scp} \tag{23}$$

Thus the elastic moduli of the solid cement paste can be determined by solving Eqs. (21)–(23) simultaneously. With K_{scp}, G_{scp}, E_{scp}, and ν_{scp} known, the elastic moduli of each ITZ shell element and the bulk paste are obtained from Eqs. (17)–(20). Thus, the elastic moduli of concrete can be evaluated by solving the *n*-layered spherical inclusion problem as follows:

(1) At step 1, composite sphere 1 is considered, in which the spherical aggregate is the inclusion phase, ITZ shell element 1 is the matrix phase, and the volume fraction of the inclusion phase is r_a^3/r_1^3. Thus, the elastic moduli of composite sphere 1 are obtained from Eqs. (17)–(20).
(2) At step i ($i = 2, 3, \ldots, p$), composite sphere i is considered, in which composite sphere $(i - 1)$ is the inclusion phase, ITZ shell element i is the matrix phase, and the volume fraction of the inclusion phase is r_{i-1}^3/r_i^3. Thus, the elastic moduli of composite sphere i are obtained from Eqs. (17)–(20).

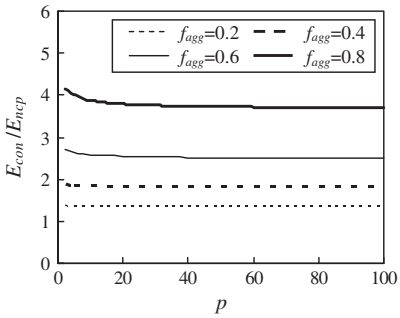

Fig. 4. Effect of the number of ITZ elements on E_{con}/E_{ncp}.

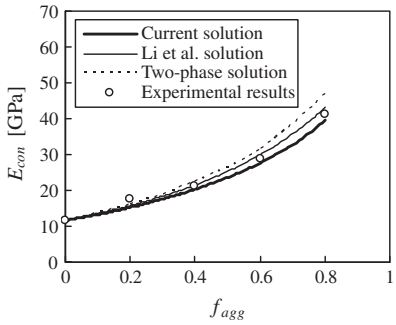

Fig. 5. Comparison of numerical results and experimental results of Stock et al. [1].

(3) At step $p+1$, composite sphere $p+1$ (i.e., concrete) is considered, in which composite sphere p is the inclusion phase, the bulk paste shell is the matrix phase, and the volume fraction of the inclusion phase is r_b^3/r_c^3. Thus, the elastic moduli K_{con}, G_{con}, E_{con}, and v_{con} of concrete are obtained from Eqs. (17) and (20).

Before the proposed model is applied to concrete, it is necessary to evaluate the effect of the number of ITZ shell elements, p on the simulation. Obviously, dividing the ITZ into more elements will improve the accuracy of the simulation, but at the cost of longer computation time. For this purpose, the Fuller gradation is considered and $w_0/c = 0.5$, $D_1 = 0.15$ mm, $D_{L+1} = 16$ mm, $h = 0.03$ mm, $t = 28$ days, $v_{ncp} = 0.25$, $E_{agg}/E_{ncp} = 10$, and the Poisson's ratio of aggregate $v_{agg} = 0.15$. Fig. 4 shows the relationship between E_{con}/E_{ncp} and p. It can be seen from Fig. 4 that E_{con}/E_{ncp} decreases monotonically with p up to about $p = 70$. For $p > 70$, E_{con}/E_{neat} achieves a relatively stable value, which suggests that the minimum number of ITZ shell elements is about 70. The convergency speed decreases with the increase of f_{agg}. Similar trends appear for larger E_{agg}/E_{ncp} and f_{agg} values. As a conservative estimate, we will use $p = 80$ for all the subsequent simulations. When $p = 1$, the ITZ layer is assumed to be uniform and the elastic moduli are approximated by the values at a distance of $h/2$ from the aggregate surface. Fig. 4 shows that, when $f_{agg} = 0.8$, E_{con}/E_{ncp} at $p = 1$ is larger than that at $p = 80$ by 12.11%. This demonstrates that the initial cement gradient at the ITZ has a significant influence on the E_{con}/E_{ncp} especially for larger f_{agg} values.

5. Model verification and discussions

5.1. Comparison with experimental results

For the purpose of verification, three independent sets of experimental data are selected: two were collected from the literature and one was obtained from the self-conducted experiment.

The first one is taken from Stock et al. [1]. In their experiment, the aggregate gradation was taken from the grading curve 3 of British Road Research Laboratory, the maximum and minimum aggregate diameters were 19 and 0.15 mm, respectively, and the aggregate volume fraction was from 0.2 to 0.8. The overall water/cement ratio was 0.5. The Young's moduli of aggregate and neat cement paste were 74.5 and 11.6 GPa, respectively. A good aggregate distribution was achieved by sealing each mold with a top plate after initial compaction and then vibrating the assembly with the top plate in various positions relative to the vibrating table. The Young's moduli of concretes with different aggregate volume fractions were measured as shown in Fig. 5. To compare with the experimental results, the Poisson's ratios of aggregate and neat cement paste, and the ITZ thickness are needed, but this information was not provided in their experiment. To make the comparison feasible, it can be reasonably estimated from the research literature. According to Li et al. and Simeonov and Admad [6,25], the Poisson's ratios for aggregate and neat cement paste can be taken as: $v_{agg} = 0.15$ and $v_{neat} = 0.25$. In studying the effect of aggregate surface on the distribution of cement grains, Zheng et al. found from the simulation results that the ITZ thickness varies from 0.01 mm to 0.05 mm for normal strength concrete [26]. Thus in the verification, h takes the average, i.e., $h = 0.03$ mm. With the values of these variables known, the Young's modulus of concrete can be calculated by solving the n-layered spherical inclusion problem. The results are shown in Fig. 5. The relative error for aggregate volume fraction, $f_{agg} = 0.2$, 0.4, 0.6, and 0.8, is 14.44%, 5.13%, 4.74%, and 4.32%, respectively. Obviously, when the aggregate volume fraction is greater than 0.4, the difference between the experimental results and the numerical results is small. When the aggregate volume fraction is small ($f_{agg} = 0.2$), the proposed model underestimates the Young's modulus of concrete. Fortunately, the aggregate volume fraction in most concrete of practical use is usually around 0.7 and certainly larger than 0.4. In Fig. 5, the two-phase solution and the Li et al. (three-phase) solution [6] are also given for comparison. It can be seen from Fig. 5 that, the two-phase solution obviously overestimates the Young's modulus of concrete due to the neglect of the ITZ. The Li et al. solution is also in good agreement with the experimental results with an average relative error of 4.89% but is larger than the current solution by 3.32%, 5.59%, 8.34%, and 8.91% for a given value of f_{agg} at 0.2, 0.4, 0.6, and 0.4, respectively. The overestimate could be induced by the assumption of uniform ITZ layer. This implies that the Li et al. solution is equivalent to the current solution for $p = 1$ and therefore slightly larger than the current solution for $p = 80$ as seen from Fig. 4.

The second one is taken from Wang et al. [2]. In their experiment, ASTM Portland cement, Type I/II, and screened silica Ottawa sand (20–30) were used. The maximum and minimum aggregate diameters were 0.84 and 0.59 mm, respectively [5]. The overall water/cement ratio was 0.30. The Young's moduli and Poisson's ratios of aggregate and neat cement paste were as follows: $E_{agg} = 86.70$ GPa, $E_{neat} = 30.13$ GPa, $v_{agg} = 0.17$, and $v_{neat} = 0.28$. The ITZ thickness was again not provided and hence taken to be the same value as in the previous verification, i.e., $h = 0.03$ mm. With these data, the Young's modulus of concrete can be evaluated and compared with the experimental results of Wang et al. as shown in Fig. 6. It can be seen from Fig. 6 that the numerical results are in good agreement with the experimental results. The relative error between them for aggregate volume fraction, $f_{agg} = 0.15$, 0.27, 0.40, 0.52, and 0.65, is 0.32%, 1.91%, 3.04%, 5.31%, and 2.05%, respectively. The two-phase solution and Li et al. solution are again shown in Fig. 6. As can be seen from Fig. 6, the two-phase solution overestimates the Young's modulus of concrete. The Li et al. solution is in good agreement with the experimental results with an average relative error of 2.19% but is larger than the current

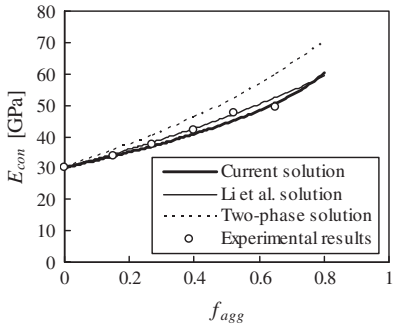

Fig. 6. Comparison of numerical results and experimental results of Wang et al. [2].

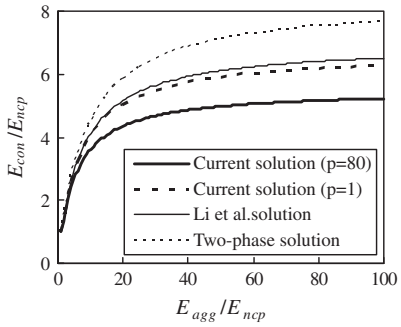

Fig. 8. Comparison of various numerical methods.

solution by 2.07%, 3.34%, 4.28%, 4.55%, and 3.61% for a given value of f_{agg} at 0.15, 0.27, 0.40, 0.52, and 0.65, respectively.

The third one is obtained from the self-conducted experiment. In this experiment, concrete specimens of water/cement ratios 0.4, 0.5, and 0.6 were cast using an ordinary Portland cement (equivalent to ASTM Type I Portland cement) produced in Huangshi, China. The Fuller gradation was adopted, the aggregate volume fraction was fixed at 0.7, and the minimum and maximum aggregate diameters were 0.15 and 16 mm, respectively. At the same time, neat cement paste specimens with a water/cement ratio of 0.5 were cast using the same cement for experimental calibration. After these specimens were cured in water at 21 °C for 28 days, the elastic moduli were measured as follows: E_{agg} = 68.9 GPa, E_{neat} = 17.8 GPa, v_{agg} = 0.15, v_{neat} = 0.25, and the Young's modulus of concrete is plotted against the water/cement ratio in Fig. 7. As in the first verification, the ITZ thickness is taken as 0.03 mm. With these data, the Young's modulus of concrete can be estimated as shown in Fig. 7. Fig. 7 again shows that the numerical results are in good agreement with the experimental results. The relative error between them for water/cement ratio, w_0/c = 0.4, 0.5, and 0.6, is 0.30%, 1.11%, and 1.74%, respectively. To obtain the Li et al. solution, the Young's moduli of neat cement paste with water/cement ratios of 0.4 and 0.6 were measured as 21.9 GPa and 15.2 GPa, respectively. Thus, the two-phase solution and Li et al. solution are given in Fig. 7. Fig. 7 shows that, on average, the two-phase solution and Li et al. solution overestimate the Young's modulus of concrete by 14.93% and 8.62%, respectively. Therefore, the validity of the n-layered spherical inclusion model proposed in this paper is verified.

5.2. Comparison with other models

To further compare various solutions for the elastic moduli of concrete, the Fuller gradation is considered and f_{agg} = 0.75, D_1 = 0.15 mm, D_{L+1} = 16 mm, w_0/c = 0.5, h = 0.03 mm, and t = 28 days. The results are shown in Fig. 8. It can be seen from Fig. 8 that, since the ITZ is neglected, the two-phase solution is larger than the other solutions for a given value of E_{agg}/E_{ncp}. The Li et al. solution is very close to the current solution for p = 1 since the ITZ layer is both assumed to be uniform in the two solutions. For a given E_{agg}/E_{ncp}, the Li et al. solution is always larger than the current solution for p = 80 and the discrepancy between them increases with an increase in E_{agg}/E_{ncp}. Specifically, the Li et al. solution is larger than the current solution for p = 80 by 8.57%, 13.80%, 18.49%, 23.27%, and 24.49% for a given value of E_{agg}/E_{ncp} at 5, 10, 20, 60, and 100, respectively. This again shows that the initial cement gradient has a significant influence on the elastic moduli of concrete especially for large f_{agg} and/or E_{agg}/E_{ncp} .

5.3. Sensitivity analysis

As can be seen from the proposed n-layered spherical inclusion model, the main factors that affect the elastic moduli of concrete include the maximum aggregate diameter, aggregate gradation, and ITZ thickness. It is therefore of practical significance to quantify these influential factors through sensitivity analysis. Since the aggregate volume fraction is around 0.75 for normal concrete, f_{agg} is taken as 0.75. In addition, D_1 = 0.15 mm, v_{agg} = 0.15, v_{neat} = 0.25, t = 28 days, w_0/c = 0.5, and the Young's moduli of concrete and aggregate are both normalized by the Young's modulus of neat cement paste with a water/cement ratio of 0.5 in all the following computations.

To investigate the effect of the maximum aggregate diameter on the relative Young's modulus of concrete, let h = 0.03 mm, and D_{L+1} = 8 mm, 16 mm, and 24 mm, respectively. The results are shown in Fig. 9 for the Fuller gradation, which clearly shows that the relative Young's modulus of concrete increases with the increase of D_{L+1}. Specifically, when D_{L+1} increases from 8 mm to 24 mm, E_{con}/E_{ncp} increases by 8.78%, 10.48%, and 10.89% for a given value of E_{agg}/E_{ncp} at 20, 60, and 100, respectively. The reason for

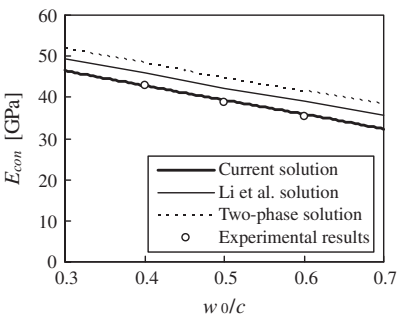

Fig. 7. Comparison of numerical results and self-conducted experimental results.

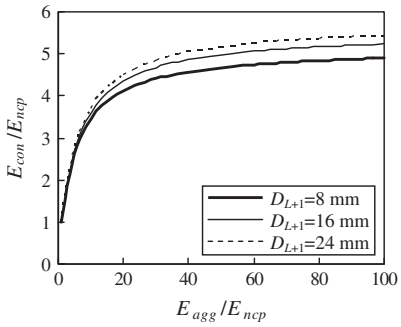

Fig. 9. Effect of maximum aggregate diameter on relative Young's modulus of concrete.

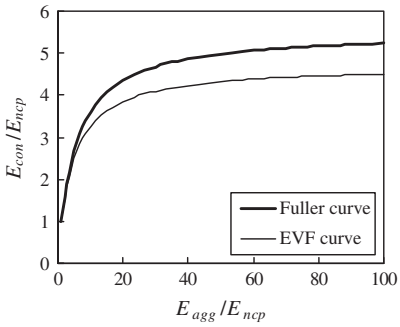

Fig. 10. Effect of aggregate gradation on relative Young's modulus of concrete.

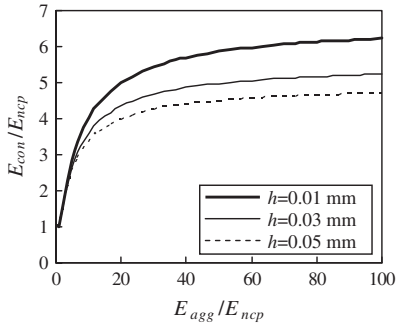

Fig. 11. Effect of ITZ thickness on relative Young's modulus of concrete.

this is that the aggregate surface area decreases relatively as the maximum aggregate diameter increases, which will reduce the ITZ volume fraction.

As for the effect of the aggregate gradation on the relative Young's modulus of concrete, let $h = 0.03$ mm and $D_{L+1} = 16$ mm. The results are shown in Fig. 10 for the Fuller gradation and the equal volume fraction (EVF) gradation [7]. From Fig. 10 it can be seen that, for a given E_{agg}/E_{ncp}, the relative Young's modulus of concrete with the Fuller gradation is always larger than that with the EVF gradation. The Young's modulus of concrete with the Fuller gradation is larger than that with the EVF gradation by 11.60%, 13.45%, and 13.89% for a given value of E_{agg}/E_{ncp} at 20, 60, and 100, respectively. This is due to the fact that there are more small aggregate particles included in the EVF gradation [7], which makes the ITZ volume fraction of concrete with the EVF gradation be larger than that with the Fuller gradation for a given aggregate volume fraction. This implies that the aggregate gradation has a significant influence on the Young's modulus of concrete.

Finally, the effect of the ITZ thickness on the relative Young's modulus of concrete is shown in Fig. 11 for the Fuller gradation, where $D_{L+1} = 16$ mm, and $h = 0.01$ mm, 0.03 mm, and 0.05 mm, respectively. As expected, the relative Young's modulus of concrete decreases with the increase of the ITZ thickness for a given E_{agg}/E_{ncp}. When h increases from 0.01 mm to 0.05 mm, the relative Young's modulus of concrete decreases by 20.37%, 23.84%, and 24.67% for a given value of E_{agg}/E_{ncp} at 20, 60, and 100, respectively.

In summary, the most important factor that influences the Young's modulus of concrete is the ITZ thickness. When $E_{agg}/E_{ncp} = 60$, the relative Young's modulus of concrete at $h = 0.01$ mm is larger than that at $h = 0.05$ mm by 23.84%. The extent to which the maximum aggregate diameter and aggregate gradation influence the relative Young's modulus of concrete is respectively 10.48% and 13.45% when $E_{agg}/E_{ncp} = 60$.

It should be pointed out that the proposed n-layered spherical inclusion model has been developed for normal aggregate concrete. When part of normal aggregate is replaced with lightweight aggregate, the ITZ microstructure around the lightweight aggregate can be quite different from that around the normal aggregate due to movement of water between the lightweight aggregate and the paste [27–30]. This complicates the computation of the ITZ volume fraction and the modeling of the ITZ porosity gradient.

6. Conclusions

An n-layered spherical inclusion model has been presented in this paper for predicting the elastic moduli of concrete with inhomogeneous ITZ. Based on the stereological analysis of the aggregate size distribution, the ITZ volume fraction has been derived in an analytical manner. A semi-empirical cement gradient model has been constituted and used to estimate the local water/cement ratio, degree of hydration, and porosity at the ITZ. By dividing the ITZ into a series of homogenous concentric shell elements, the elastic moduli of concrete have been determined by solving the n-layered spherical inclusion problem. After the validity of the model has been verified with three independent sets of experimental data, the effects of the maximum aggregate diameter, aggregate gradation, and ITZ thickness on the Young's modulus of concrete have been investigated through sensitivity analysis. Based on the numerical results, it has been found that the most important factor influencing the Young's modulus of concrete is the ITZ thickness. For a given value of E_{agg}/E_{ncp} at 60, the relative Young's modulus of concrete at $h = 0.01$ mm is larger than that at $h = 0.05$ mm by 23.84%. It has also been found that, when $E_{agg}/E_{ncp} = 60$, the extent to which the maximum aggregate diameter and aggregate gradation influence the relative Young's modulus of concrete is 10.48% and 13.45%, respectively. It can be concluded that the proposed n-layered spherical inclusion model can be used to predict the elastic moduli of concrete.

Acknowledgments

The financial support from the National Basic Research Program (973 Program) with Grant No. 2009CB623200, the National Natural Science Foundation with Grant Nos. 50878196 and 50838008, and the Key Science and Technology Innovation Team of Zhejiang Province with Grant No. 2010R50034, of the People's Republic of China, is greatly acknowledged. All reviewers' constructive comments and suggestions are gratefully appreciated.

References

[1] Stock AF, Hannant DJ, Williams RIT. The effect of aggregate concentration upon the strength and modulus of elasticity of concrete. Mag Concr Res 1979;31(109):225–34.
[2] Wang JA, Lubliner J, Monteiro PJM. Effect of ice formation on the elastic moduli of cement paste and mortar. Cem Concr Res 1988;18(6):874–85.
[3] Vilardell J, Aguado A, Agullo L, Gettu R. Estimation of the modulus of elasticity for dam concrete. Cem Concr Res 1998;28(1):93–101.
[4] Garboczi EJ, Bentz DP. Analytical formulas for interfacial transition zone properties. Adv Cem Based Mater 1997;6(3–4):99–108.
[5] Lutz MP, Monteiro PJM, Zimmerman RW. Inhomogeneous interfacial transition zone model for the bulk modulus of mortar. Cem Concr Res 1997;27(7):1113–22.
[6] Li GQ, Zhao Y, Pang SS. Four-phase sphere modelling of effective bulk modulus of concrete. Cem Concr Res 1999;29(6):839–45.
[7] Li CQ, Zheng JJ, Zhou XZ, McCarthy MJ. A numerical method for the prediction of elastic modulus of concrete. Mag Concr Res 2003;55(6):497–506.
[8] Nadeau JC. A multiscale model for effective moduli of concrete incorporating ITZ water–cement ratio gradients, aggregate size distributions, and entrapped voids. Cem Concr Res 2003;33(1):103–13.
[9] Zheng JJ, Li CQ, Zhou XZ. An analytical method for prediction of the elastic modulus of concrete. Mag Concr Res 2006;58(10):665–73.
[10] Nilsen AU, Monteiro PJM. Concrete: a three phase material. Cem Concr Res 1993;23(1):147–51.

[11] Crumbie AK. Characterisation of the microstructure of concrete. PhD thesis, Imperial College London; 1994.
[12] Ollivier JP, Maso JC, Bourdette B. Interfacial transition zone in concrete. Adv Cem Based Mater 1995;2(1):30–8.
[13] Christensen RM. Mechanics of composite materials. New York: John Wiley & Sons; 1979.
[14] Devore JL. Probability and statistics for engineering and the sciences. Belmont: Duxbury Press; 1995.
[15] Lu BL, Torquato S. Nearest-surface distribution functions for polydispersed particle system. Phys Rev A 1992;45(8):5530–44.
[16] Parrot LJ, Killoh DC. Prediction of cement hydration. Br Ceram Proc 1984;35:41–53.
[17] Hansen TC. Physical structure of hardened cement paste: a classical approach. Mater Struct 1986;19(6):423–36.
[18] Duan HL, Jiao Y, Yi X, Huang ZP, Wang J. Solutions of inhomogeneity problems with graded shells and application to core–shell nanoparticles and composites. J Mech Phys Solids 2006;54(7):1401–25.
[19] Christensen RM, Lo KH. Solutions for effective shear properties in three phase sphere and cylinder models. J Mech Phys Solids 1979;27(4):315–30.
[20] Bernard O, Ulm FJ, Lemarchand E. A multiscale micromechanics-hydration model for the early-age elastic properties of cement-based materials. Cem Concr Res 2003;33(9):1293–309.
[21] Constantinides G, Ulm FJ. The effect of two types of C–S–H on the elasticity of cement-based materials: results from nanoindentation and micromechanical modelling. Cem Concr Res 2004;34(1):67–80.
[22] Šmilauer V, Bittnar Z. Microstructure-based micromechanical prediction of elastic properties in hydrating cement paste. Cem Concr Res 2006;36(9):1708–18.
[23] Coussy O. Poromechanics. New York: John Wiley & Sons; 2004.
[24] Timoshenko SP, Goodier JN. Theory of elasticity. New York: McGraw-Hill; 1970.
[25] Simeonov P, Ahmad S. Effect of transition zone on the elastic behaviour of cement-based composites. Cem Concr Res 1995;25(1):165–76.
[26] Zheng JJ, Li CQ, Zhou XZ. Characterization of the microstructure of interfacial transition zone in concrete. ACI Mater J 2005;102(4):265–71.
[27] Castro J, Keiser L, Golias M, Weiss J. Absorption and desorption properties of fine lightweight aggregate for application to internally cured concrete mixtures. Cem Concr Compos 2011;33(10):1001–8.
[28] Henkensiefken R, Bentz DP, Nantung T, Weiss J. Volume change and cracking in internally cured mixtures made with saturated lightweight aggregate under sealed and unsealed conditions. Cem Concr Compos 2009;31(7):427–37.
[29] Bentz DP. Influence of internal curing using lightweight aggregates on interfacial transition zone percolation and chloride ingress in mortars. Cem Concr Compos 2009;31(5):285–9.
[30] Elsharief A, Cohen MD, Olek J. Influence of lightweight aggregate on the microstructure and durability of mortar. Cem Concr Res 2005;35(7):1368–76.